Supplementary Information for:

Facile Synthesis of Magnetic Fluorescent Nanoparticles: Adsorption and Selective Detection of Hg(II) in Water

Lei Li,[a,b] Chao Jia,[a,b] Feijun Wang,[a,b] Honglei Fan,[c] Weizhou Jiao[c] and Ziqiang Shao*[a,b]

[a]School of Materials Science and Engineering, Beijing Institute of Technology, Beijing 100081, China

[b]Beijing Engineering Research Centre of Cellulose and Its Derivatives, Beijing 100081, China

[c]Shanxi Province Key Laboratory of Higee-Oriented Chemical Engineering, North University of China, Taiyuan 030051, China

Corresponding Author

* E-mail: shaoziqiang@263.net (Z. Shao)

1. Parameters of the IS-RPB equipment.

Table S1. Parameters of the IS-RPB equipment.

Packing material	Stainless steel wire meshes
Stainless steel wire meshes diameter	0.275 mm
Shell diameter	200 mm
Diameter of pipe distributor	10 mm
Outer diameter of packing	160 mm
Inner diameter of packing	60 mm
Axial height of packing	60 mm

2. pH stability of adsorbent-chemosensor

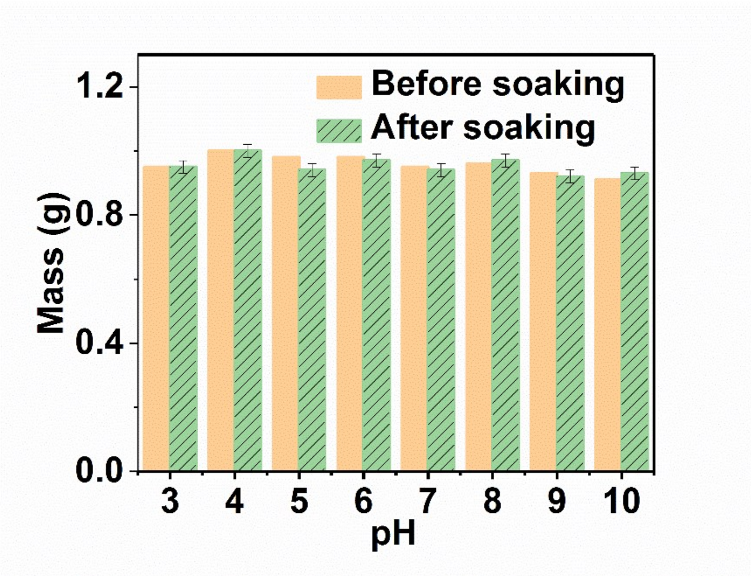

Fig. S1. The stability of the adsorbent-chemosensor under different pH values.

2. Recovery ability of the adsorbent-chemosensor.

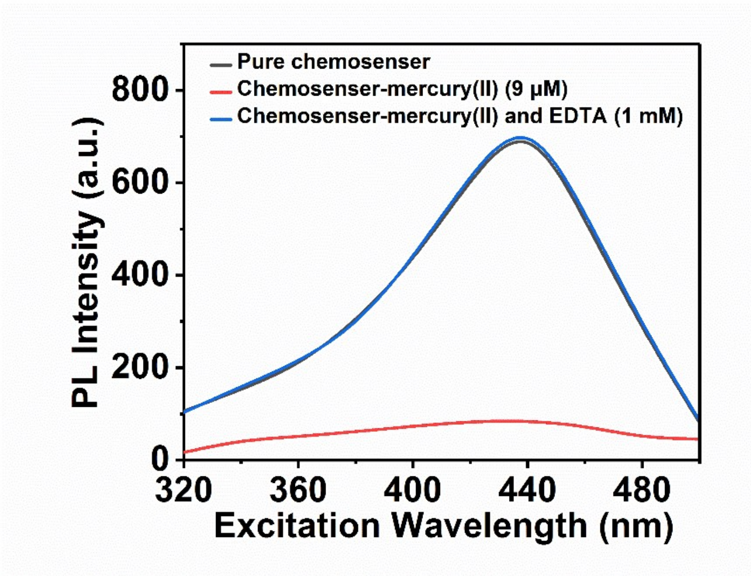

Fig. S2. The PL spectra of different chemosensor systems.

3. Recognition mercury(II) ability of the adsorbent-chemosensor in real water.

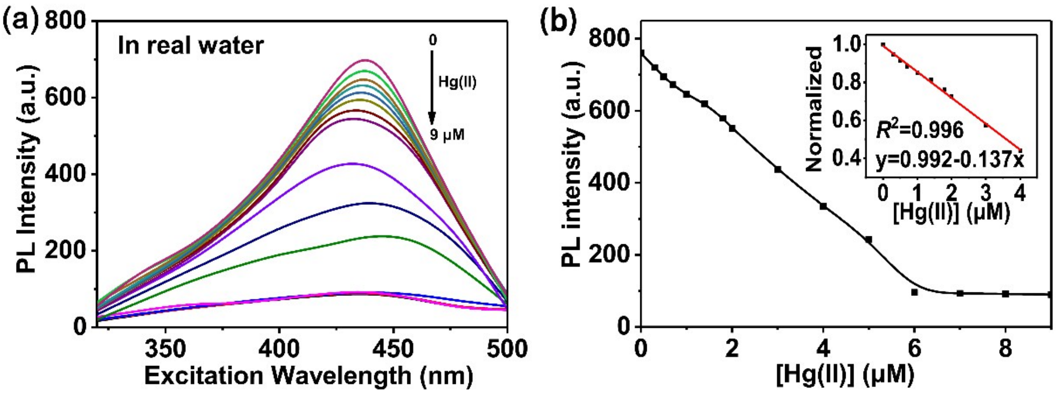

Fig. S3. (a) Fluorescence spectra of Fe_3O_4@CS/CQDs@CQDs at different Hg(II) concentrations of 0-9 μM in real water. (b) Corresponding maximum fluorescence intensity values (440 nm) for different Hg(II) concentrations. Inset is the linear fitting plot of fluorescence intensities for Fe_3O_4@CS/CQDs@CQDs (0.1 g L^{-1}) as a function of Hg(II) concentration (0-4×10^{-6} M). The real water sample was collected from the lake in the old summer palace.

4. Comparison of different fluorescent probe for mercury detection.

Table S2. Comparison of different fluorescent probe for mercury detection.

Detection method	LOD	Linear range
Au filter membrane[1]	1.16 nM	0-11 μM
Rhodamine derivative functionalized chitosan[2]	3.42 μM	0-6 μM
Mesoporous silica nanocomposites[3]	2 nM	0-50 nM
Fe_3O_4@SiO_2–Au@$PSiO_2$[4]	20 nM	0-0.75μM
DNA-Functionalized hydrogels[5]	10 nM	0-200 nM
CNPs[6]	42 nM	0.25-12 μM
N, S-GQDs[7]	0.14 nM	0.001–15 mM
Magnetic self-assembled zeolite clusters[8]	0.32 μM	1-6 μM
DNA-functionalized-graphene[9]	0.82 ng/mL	1-20 ng/mL
S-CQDs[10]	2 nM	0.02-2 μM
Our study	12.43 nM	0-4 μM

5. Langmuir isotherm model linear fitting process.

As in Eq. (S1) shows the Langmuir isothermal adsorption equation[11], which represents the relationship between q_e and c_e. Eq. (S1) can be transformed into Eq. (S2), one can see that the c_e/q_e has a linear relationship with c_e. Table S1 display the fitting results.

$$q_e = \frac{q_m K_L c_e}{1 + K_L c_e} \tag{S1}$$

$$\frac{c_e}{q_e} = \frac{1}{q_m K_L} + \frac{c_e}{q_m} \tag{S2}$$

Where q_e is the equilibrium adsorbing amount of Hg (II) ion, q_m is the maximum adsorption capacity that corresponds to complete monolayer coverage, K_L is the equilibrium constant, and c_e is the equilibrium concentration of the Hg (II) ion solution.

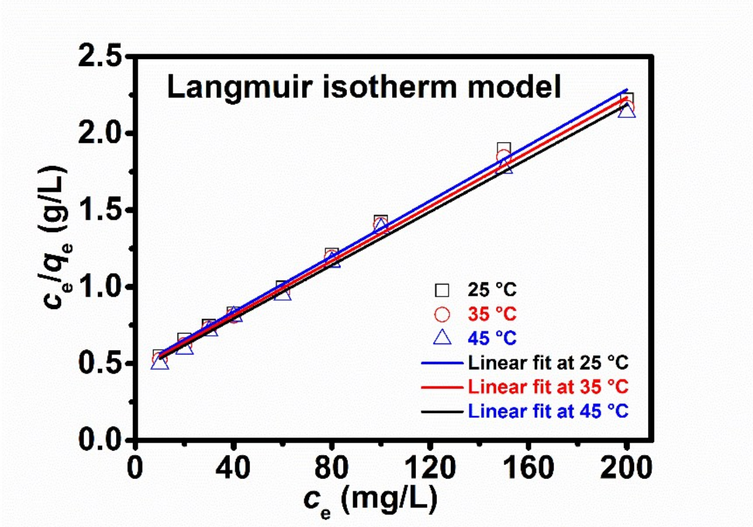

Fig. S4. Liner fitting results of Langmuir isothermal adsorption.

Table S3. Fitting equations of Langmuir isothermal adsorption equation.

T (°C)	Regression equation
25	c_e/q_e= 0.476+0.00905 c_e
35	c_e/q_e = 0.460+0.00887 c_e
45	c_e/q_e = 0.446+0.00870 c_e

6. Freundlich isotherm model linear fitting process.

As in Eq. (S3) shows the Freundlich isothermal adsorption equation [12], which represents the relationship between q_e and c_e. Eq. (S3) can be transformed into Eq. (S4), one can see that the log q_e has a linear relationship with log c_e. Table S2 display the fitting results.

$$q_e = k_F c_e^{\frac{1}{n}} \tag{S3}$$

$$log q_e = log k_F + \frac{1}{n} log c_e \tag{S4}$$

Where q_e is the equilibrium adsorbing amount of Hg (II) ion, q_m is the maximum adsorption capacity, k_F and n is the Freundlich constant, and c_e is the equilibrium concentration of the Hg (II) ion solution.

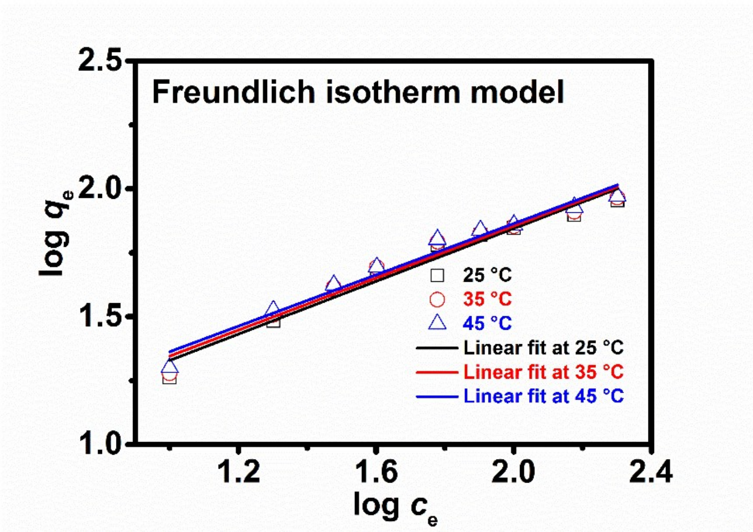

Fig. S5. Liner fitting results of Langmuir isothermal adsorption.

Table S4. Fitting equations of Freundlich isothermal adsorption equation

T (°C)	Regression equation
25	$\log q_e = 0.813+0.516 \log c_e$
35	$\log q_e = 0.837+0.509 \log c_e$
45	$\log q_e = 0.862+0.501 \log c_e$

7. Thermodynamic parameters.

The Gibbs free energy change of adsorption process is calculated by following equation:

$$\Delta G = -RT\ln\frac{q_e}{c_e} \tag{S5}$$

$$\frac{q_e}{c_e} = \lim_{c_{el}\to 0}\frac{c_{es}}{c_{el}} \tag{S6}$$

where R is the gas constant (8.314 J mol^{-1} K^{-1}), T is an absolute temperature (K) and k_c is the adsorption equilibrium constant. c_{es} and c_{el} are the values of solid and liquid phase concentration in equilibrium (mg L^{-1}) respectively. The relationship between the equilibrium constant (k_c) and temperature is given by the Van't Hoff equation Eq. (S7).

$$\ln\frac{q_e}{c_e} = \frac{\Delta S}{R} - \frac{\Delta H}{RT} \tag{S7}$$

The entropy change of adsorption (ΔS) and the enthalpy change of adsorption(Δh) are obtained from the slope and intercept of a Van't Hoff plot of ln q_e/c_e versus $1/T$ (Fig. S5).

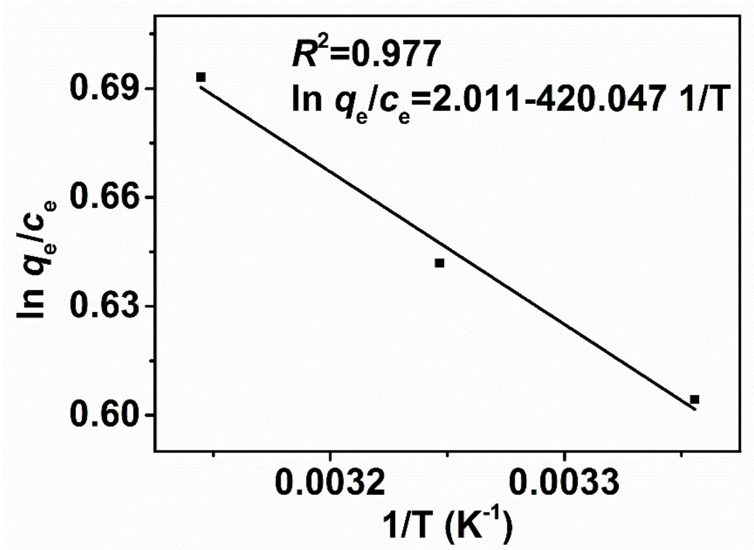

Fig. S6. Liner fitting results of Van't Hoff equation.

8. Adsorption kinetic models.

The pseudo-first-order kinetic model is given as:

$$q_t = q_e(1 - exp(- k_1)) \tag{S8}$$

where q_t and q_e (mg g^{-1}) are the adsorption capacity at time t and equilibrium time, respectively. k_1 (min^{-1}) is the pseudo-first order model rate constant. Eq. S8 can be transformed into Eq. S9, one can see that the ln(q_e-q_t) has a linear relationship with t. Fig. S7 display the fitting results.

$$\ln (q_e - q_t) = \ln q_e - k_1t \tag{S9}$$

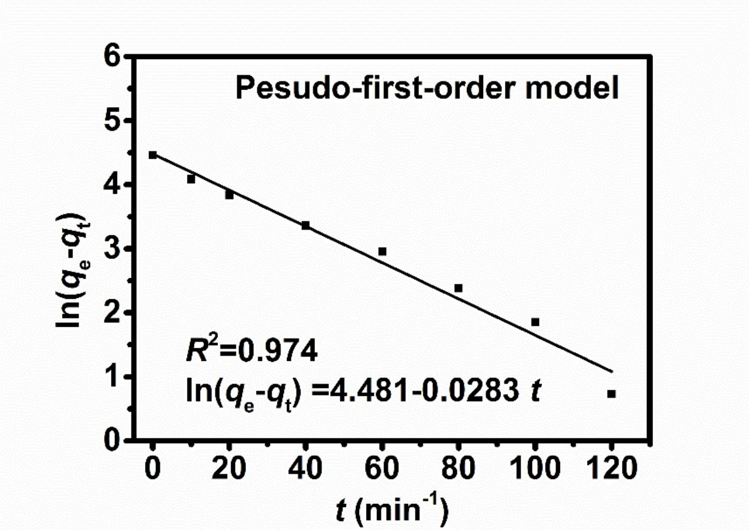

Fig. S7. Liner fitting results of pseudo-first-order kinetic model.

The pseudo second order kinetic model by Ho and McKay is given as [13]:

$$q_t = \frac{k_2 q_e^2 t}{1 + k_2 q_e t} \tag{S10}$$

where k_2 (g mg^{-1} min^{-1}) is the adsorption rate constant. Eq. (E11) can be transformed into Eq. (S10), one can see that the t/q_t has a linear relationship with t. Fig. S8 display the fitting results:

$$\frac{t}{q_t} = \frac{1}{k_2 q_e^2} - \frac{1}{q_e} t \tag{S11}$$

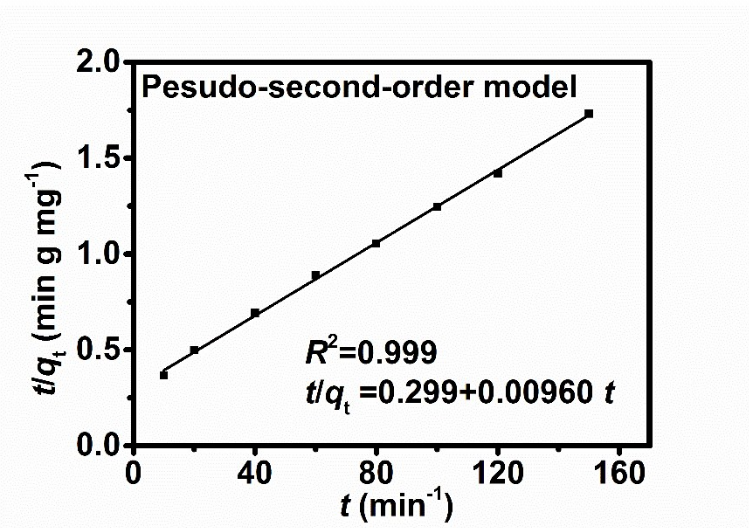

Fig. S8. Liner fitting results of pseudo-second-order kinetic model.

The intraparticle diffusion model is given as:

$$q_t = k_i t^{1/2} + C \tag{S12}$$

where k_i ((mg/g min) is the Intraparticle diffusion adsorption rate constant. One can see that the q_t has a linear relationship with $t^{1/2}$. Fig. S9 display the fitting results,

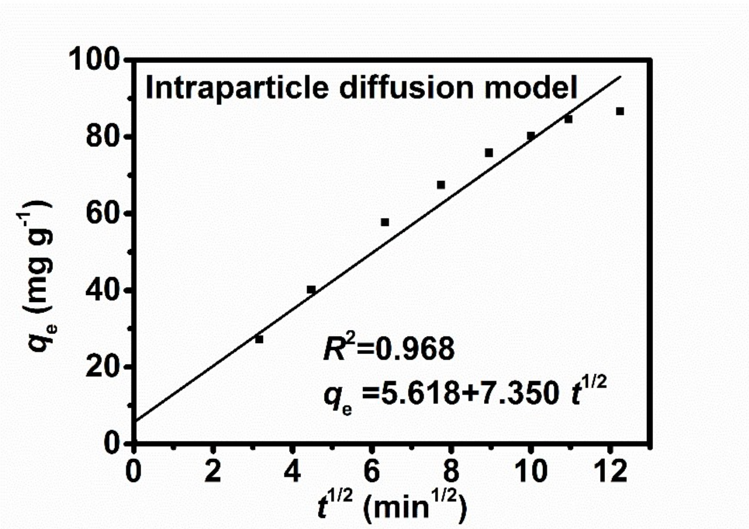

Fig. S9. Liner fitting results of intraparticle diffusion model.

Table S5 Sorption capacity of Hg (II) onto the different adsorbents.

Adsorbents	Adsorption capacities (mg/g)
Magnetic iron oxide nanoparticle[14]	0.125
Chitosan coated magnetic nanoparticles[15]	10.00
Palm shell activated carbon[16]	83.33
SS-Z[17]	42.60
Graphene/Biochar composite[18]	0.853
Polymer chemosensor[19]	5.6
Fe_3O_4@CS/CQDs/CQDs (Our study)	86.640

References

1. G. Chen, J. Hai, H. Wang, W. Liu, F. Chen and B. Wang, *Nanoscale*, 2017, **9**, 3315-3321.
2. D. Shi, F. Yan, M. Wang, Y. Zou, T. Zheng, X. Zhou and L. Chen, *Mater. Res. Bull.*, 2015, **70**, 958-964.
3. D. He, X. He, K. Wang, Y. Zhao and Z. Zou, *Langmuir*, 2013, **29**, 5896-5904.
4. Q. Lv, G. Li, Z. Cheng, H. Lu and X. Gao, *Environ. Sci. Process Impacts*, 2014, **16**, 116-123.
5. N. Dave, M. Y. Chan, P.-J. J. Huang, B. D. Smith and J. Liu, *J. Am. Chem. Soc.*, 2010, **132**, 12668-12673.

6. M. Lan, J. Zhang, Y. S. Chui, P. Wang, X. Chen, C. S. Lee, H. L. Kwong and W. Zhang, *ACS Appl Mater Interfaces*, 2014, **6**, 21270-21278.
7. N. T. N. Anh, A. D. Chowdhury and R.-a. Doong, *Sensors Actuators B: Chem.*, 2017, **252**, 1169-1178.
8. M. Yin, Z. Li, Z. Liu, X. Yang and J. Ren, *ACS Appl. Mater. Interfaces*, 2012, **4**, 431-437.
9. Y. Liu, X. Wang and H. Wu, *Biosens. Bioelectron.*, 2017, **87**, 129-135.
10. S. Yang, J. Sun, X. Li, W. Zhou, Z. Wang, P. He, G. Ding, X. Xie, Z. Kang and M. Jiang, *J. Mater. Chem. A*, 2014, **2**, 8660.
11. I. Langmuir, *J. Am. Chem. Soc.*, 1916, **38**, 2221-2295.
12. H. Freundlich, *J. Phys. Chem.*, 1906, **57**, 385-471.
13. Y. S. Ho and G. McKay, *Process Biochem.*, 1999, **34**, 451-465.
14. E. S. Cho, J. Kim, B. Tejerina, T. M. Hermans, H. Jiang, H. Nakanishi, M. Yu, A. Z. Patashinski, S. C. Glotzer, F. Stellacci and B. A. Grzybowski, *Nat. Mater.*, 2012, **11**, 978-985.
15. S. Nasirimoghaddam, S. Zeinali and S. Sabbaghi, *J. Ind. Eng. Chem.*, 2015, **27**, 79-87.
16. A. A. Ismaiel, M. K. Aroua and R. Yusoff, *Chem. Eng. J.*, 2013, **225**, 306-314.
17. F.-S. Zhang, J. O. Nriagu and H. Itoh, *Water Res.*, 2005, **39**, 389-395.
18. J. Tang, H. Lv, Y. Gong and Y. Huang, *Bioresour. Technol.*, 2015, **196**, 355-363.
19. S. Vallejos, J. A. Reglero, F. C. García and J. M. García, *J. Mater. Chem. A*, 2017, **5**, 13710-13716.